University of Strathclyde Glasgow

Strathprints Institutional Repository

Orr, P. and Niewczas, Pawel and Dysko, Adam and Booth, Campbell (2009) *FBG-based fibre-optic current sensors for power systems protection : laboratory evaluation.* In: The 44th International Universities' Power Engineering Conference, 2009-09-01 - 2009-09-04, Glasgow.

Strathprints is designed to allow users to access the research output of the University of Strathclyde. Copyright © and Moral Rights for the papers on this site are retained by the individual authors and/or other copyright owners. You may not engage in further distribution of the material for any profitmaking activities or any commercial gain. You may freely distribute both the url (http://strathprints.strath.ac.uk/) and the content of this paper for research or study, educational, or not-for-profit purposes without prior permission or charge.

Any correspondence concerning this service should be sent to Strathprints administrator: mailto:strathprints@strath.ac.uk

http://strathprints.strath.ac.uk/

FBG-based fibre-optic current sensors for power systems protection: Laboratory evaluation

Philip Orr, Paweł Niewczas, Adam Dyśko, Campbell Booth
Institute for Energy and Environment, University of Strathclyde, Glasgow, UK, G1 1XW
E-mail: philip.orr@eee.strath.ac.uk

***Abstract*-We demonstrate experimentally for the first time an all-optical in-fibre differential current unit protection scheme utilising hybrid fibre-optic current and voltage sensors. The prototype system does not require a secondary communications channel and can interrogate up to 30 separate transducers for current and temperature at kHz rates. The scheme is shown to perform well over a range of internal and external faults indicating its ability to implement future novel protection schemes, discussed herein.**

***Index Terms*—fibre Bragg gratings, optical current sensors, protection systems, optical fibre sensors, unit protection, distance protection**

I. Introduction

Conventional differential current unit protection schemes rely on a pair of electronic protection relays that measure current phasors separately at the boundaries of the protected zone. The scheme requires a separate, often optical, communications channel for the sharing of measurement information to enable the timely identification of and reaction to internal faults [1].

The high voltage environment that the transducers must operate in poses a number of engineering problems stemming from the need for electrical isolation and requirement for transformation of high primary system current magnitudes. Additionally, when either the number of relays or distance between relays is increased, timing problems can arise due to the limited bandwidth, speed and changeable latencies of the communication channels and the increased computation requirements.

Fibre-optical sensor systems are maturing as a technology and offer a number of advantages over conventional electronic sensor regimes, including the possession of inherent electrical isolation, chemical inertness, immunity to electromagnetic interference, and their small size and serial multiplexing capability. Fibre sensor systems are therefore experiencing increased uptake in industries that operate in harsh environments, such as oil or gas, or where application-specific requirements such as large step-out distances or resistance to radiation prohibit the use of electronic sensors [2,3].

In this paper, we detail a fibre Bragg grating (FBG) based solution to wide area measurement of voltage and current for protection applications. We demonstrate experimentally the performance of the protection scheme in differential current configuration, and thereafter discuss novel protection applications of the system.

II. Hybrid Fibre-Optic Current Sensor

The Institute for Energy and Environment has developed fibre-optic point sensors for voltage and electrical current, based on fibre Bragg grating (FBG) technology, that have been applied successfully to power systems diagnostics [4]. The distributed point sensor system interrogates up to 30 separate in-fibre transducers in series, each of which is less than 30 mm in length. The transducers are constructed using a stack of bonded piezoelectric elements, each of which stretches or contracts proportionally to a voltage that is applied to external electrodes as illustrated in Figure 1.

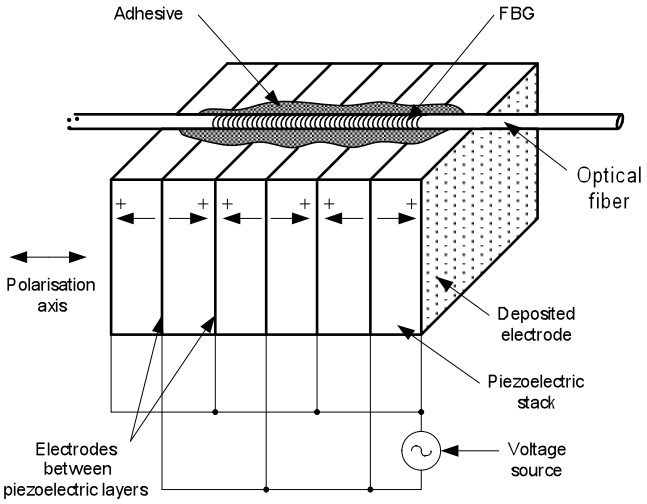

Fig. 1. Architecture of the hybrid voltage sensor element, comprising an FBG bonded to a stack of piezoelectric elements.

By bonding the FBG to the stack, such that it is in parallel to the applied electric field, the optical grating will undergo straining with the stack causing its peak reflected wavelength, the Bragg wavelength, to shift with applied voltage. An optical interrogation system, situated at the addressing end of the fibre, is then able to identify and track these peak reflected wavelengths and hence derive the applied voltage on the point sensors.

Using a small high-frequency current transformer (CT) it is possible to convert the primary current level into a voltage detectable by this transducer. Therefore, the technology is applicable to both voltage and current sensing through a similar measurement technique. This CT-based current sensor architecture is illustrated in Figure 2 below.

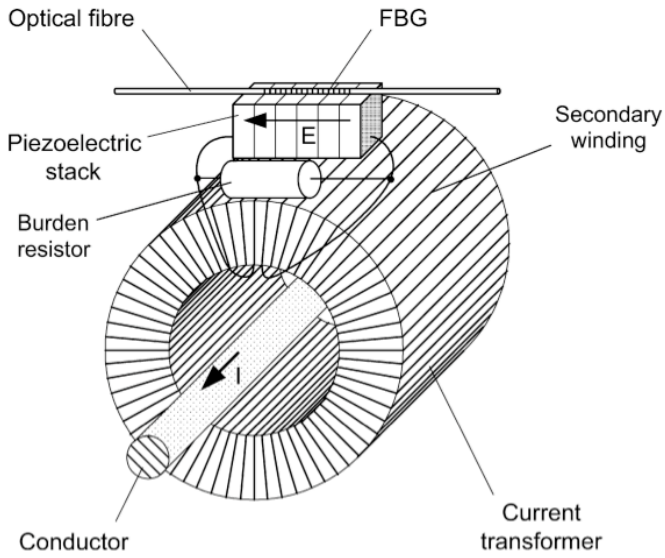

Fig. 2. CT-based optical current sensor for use with fibre Bragg grating interrogation system.

The CT transforms down the primary current into a secondary current such that a voltage is developed across the terminals of a burden resistor. This voltage is simultaneously applied to the piezoelectric stack. Power requirements for this approach are very low compared with conventional electronic current measurement, since here the CT is used only to develop the measurable voltage over the piezoelectric stack and a ferrite core can be used.

III. Unit Protection Prototype

Two sensors of the type described in Section II were separated optically by 24 km and configured to demonstrate the all-optical implementation of a differential current unit protection scheme as follows.

A. Optical current measurement system configuration

The fibre-optic interrogation system used in this laboratory evaluation is shown in Figure 3 below.

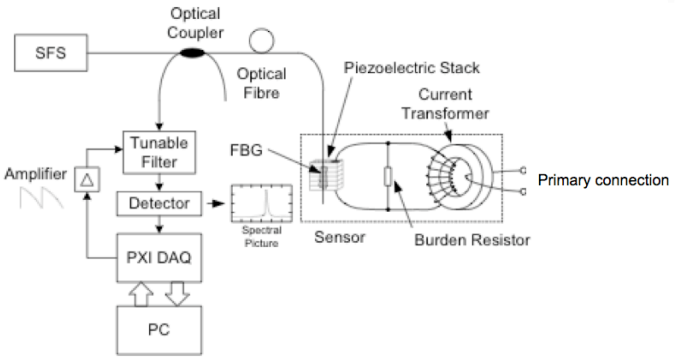

Fig. 3. Optical configuration for electrical current measurement showing fibre Bragg grating interrogation system and a single exemplary sensor measuring secondary current.

A broadband (approximately 40 nm bandwidth) super-fluorescent source, centred on the 1550 nm C-Band, illuminates a series of distant FBGs (only a single FBG shown in Figure 3). Each FBG is bonded to piezoelectric stacks as in Figure 2. Optical reflections from these sensors – transparent to each other – are guided back to the interrogator by the addressing fibre. A scanning Fabry-Perót filter is tuned at kHz rates (approximately 1.2 kHz during these tests) over the bandwidth of the source. The output of this module is photodetected by a low-noise transimpedance photodiode amplifier that is sampled continuously by the ADC hardware. Data are buffered at a National Instruments PXI unit and passed to PC-based interrogation software for construction of a spectral picture. This spectrum contains information of the peak reflections from each sensor element, which are tracked continuously such that conversion of instantaneous signals into current phasors can be performed. Retrieval of high-frequency current harmonics is also possible at this stage, potentially up to a Nyquist rate of ~5 kHz, but this capacity will not be discussed in this work.

The resolution of the current sensing system is dependent on the mating of the piezoelectric stack's operating range and the CT transforming ratio. For the prototype system, the operating range is 0 – 500 V which does not, at this stage, mate ideally with the prototype CT ratio. As such there is a noise level that can be greatly reduced by a redesign of the piezoelectric stack. Figure 4 shows the resolution of the

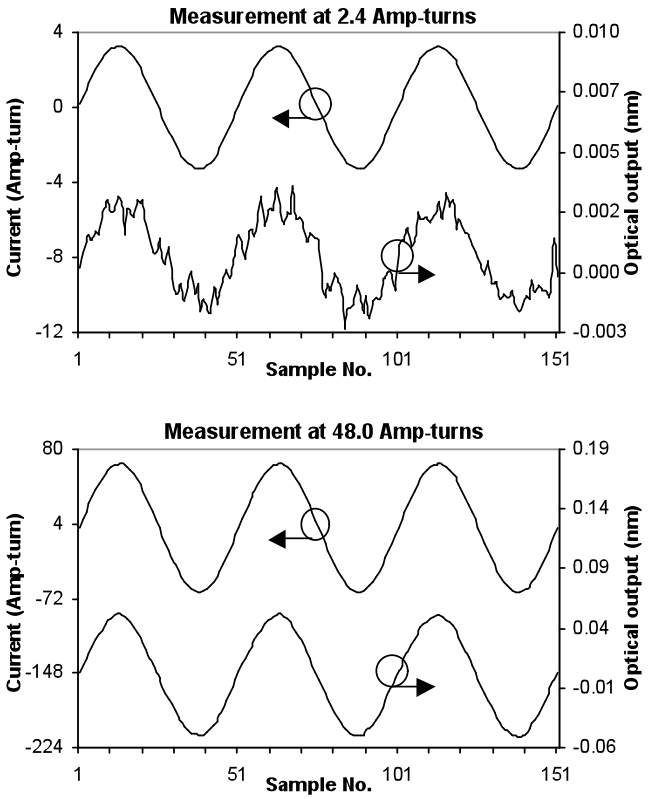

Fig. 4. Current sensor response recorded at 5% and nearly 100% of full-scale output, indicating a signal-to-noise ratio of 36 dB at full-scale output.

prototype optical current sensors recorded during initial testing.

It is important to note that the response of this sensor is sensitive also to temperature, and that therefore the optical interrogator can find both AC current and temperature simultaneously, which may have applications for plant condition monitoring using thermal measurements as input.

B. Electrical test configuration

In order to test the prototype distributed optical protection system, the measurement system described previously was configured to measure a pair of secondary currents with transducers separated optically by 24 km of singlemode fibre. The test configuration is identical to that in Figure 3 except that secondary currents are modelled using ATP and injected into the prototype test system directly via an APTS3 (Advanced Protection Testing System) unit. Figures 5 and 6 show the laboratory test configuration and prototype current sensor array respectively.

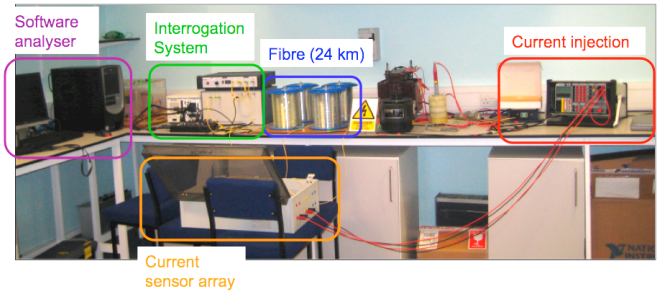

Fig. 5. Prototype differential optical protection scheme under test.

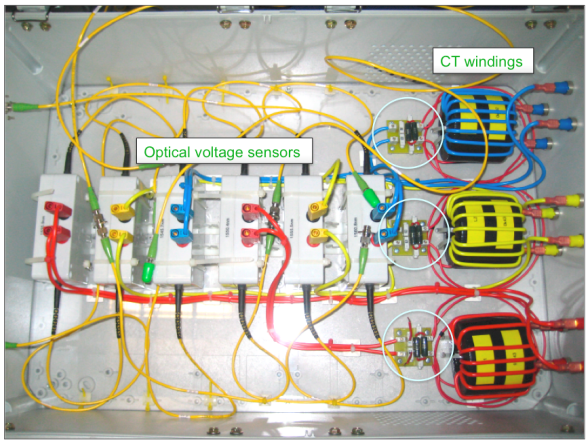

Fig. 6. Prototype optical current sensor array indicating voltage transducers, burden resistors (circled), and current transformers.

IV. Fault Testing of Optical Protection Prototype

A range of fault scenarios were simulated and input to the system. These comprised internal phase-phase and phase-earth faults through a range of resistances, and external worst-case phase-earth and 3-phase-earth faults to test the system's stability during external fault conditions.

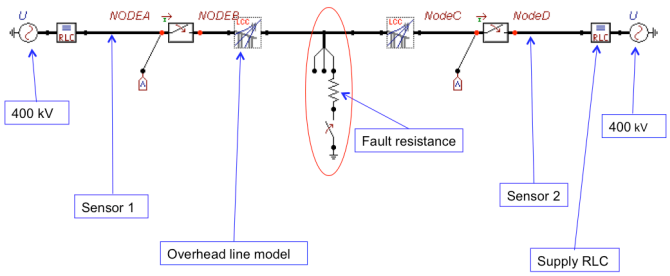

Fig. 7. Internal phase-earth fault scenario. Protected zone is region between Sensor 1 and Sensor 2. Fault is centrally placed.

A. Internal phase-earth faults

Figure 7 shows the ATP configuration used to generate secondary current data for internal phase-earth faults.

As with all faults simulated for this study, the protected zone is a region (100 km) of 400 kV transmission line, with optical sensors situated at either end of this protected zone. Internal faults are simulated in the centre of this zone through a fault resistance that is ramped from 0.1 Ω to 300 Ω, where the sensitivity of the system begins to decline, as is to be expected with biased differential protection algorithms.

The fault model produces 1 s of current data, with faulting of Phase A to earth through the fault resistance occurring at 0.5 s after initial injection. The system's response to a representative internal phase-earth fault at mid-range fault resistance (100 Ω) is shown below in Figure 8.

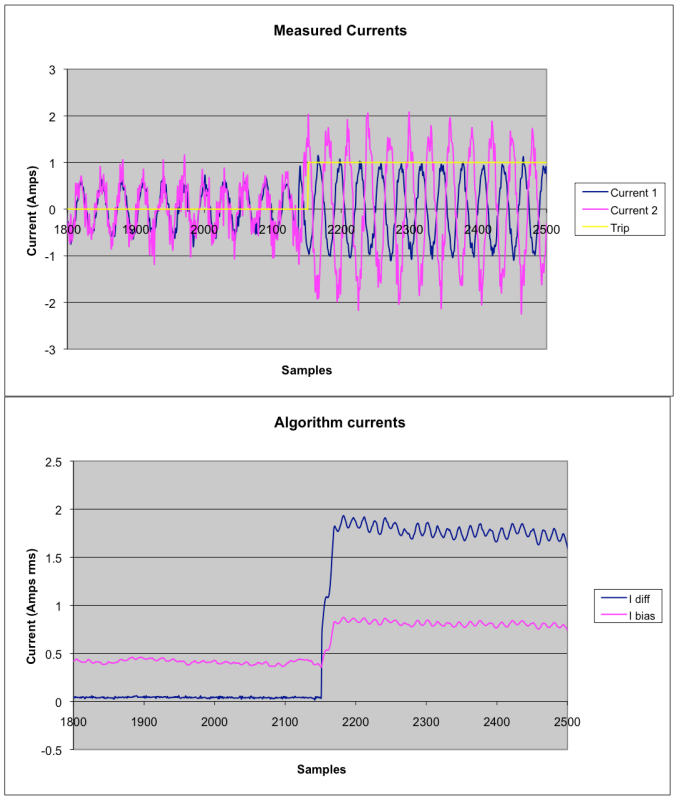

Fig. 8. Internal phase-earth fault through 100 Ω. Upper graph shows instantaneous currents and Trip comparator. Lower graph shows differential and bias currents.

For each fault resistance, up to 300 Ω, the system correctly identifies faults as indicated by the Trip comparator (yellow Boolean, Figure 8).

B. Internal phase-phase faults

Figure 9 illustrates the ATP configuration used to generate secondary current data for internal phase-phase faults.

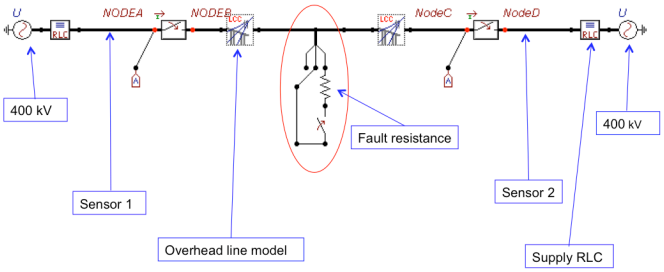

Fig. 9. Internal phase-phase fault scenario. Protected zone is region between Sensor 1 and Sensor 2. Fault is centrally placed and occurs between Phase A and Phase B.

With reference to Figure 10, which is again a representative response, this time to a phase-phase fault through 100 Ω, the system correctly identifies all internal phase-phase faults up to a fault resistance of 400 Ω.

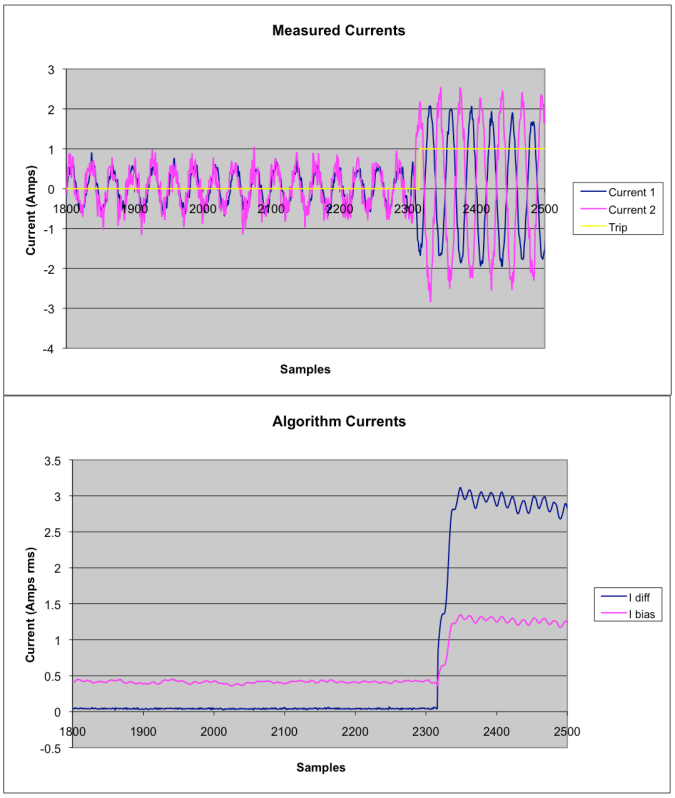

Fig. 10. Internal phase-phase fault through 100 Ω. Upper graph shows instantaneous currents and Trip comparator. Lower graph shows differential and bias currents.

C. External phase-earth faults

Figure 11 illustrates the ATP configuration used to generate secondary current data for a worst-case (lowest resistance) single phase-earth fault that is situated just outside the boundary of the protected zone.

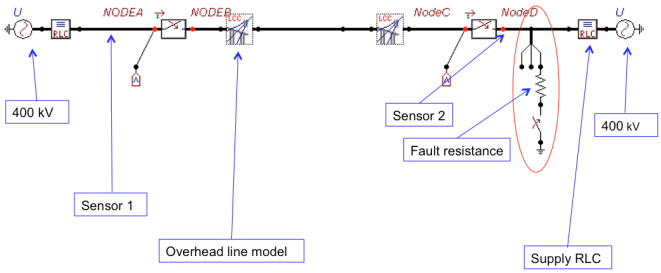

Fig. 11. External phase-earth fault scenario. Protected zone is region between Sensor 1 and Sensor 2. Fault is placed outside protected zone.

In this case, the fault resistance is set to 0.1 Ω. With reference to Figure 12, the system can be seen to avoid triggering under a worst-case phase-earth external fault. The comparator outputs 'high' for a single sample, most probably due either to capacitive discharge on the line or transient signal processing error, but this is not interpreted as a fault by the system, which in practice "waits" for six consecutive comparator "high" data points before registering a fault, as per standard protection relay design procedure. The system stability was also tested under single 3-phase-earth worst-case faults, not shown here, and found to operate correctly.

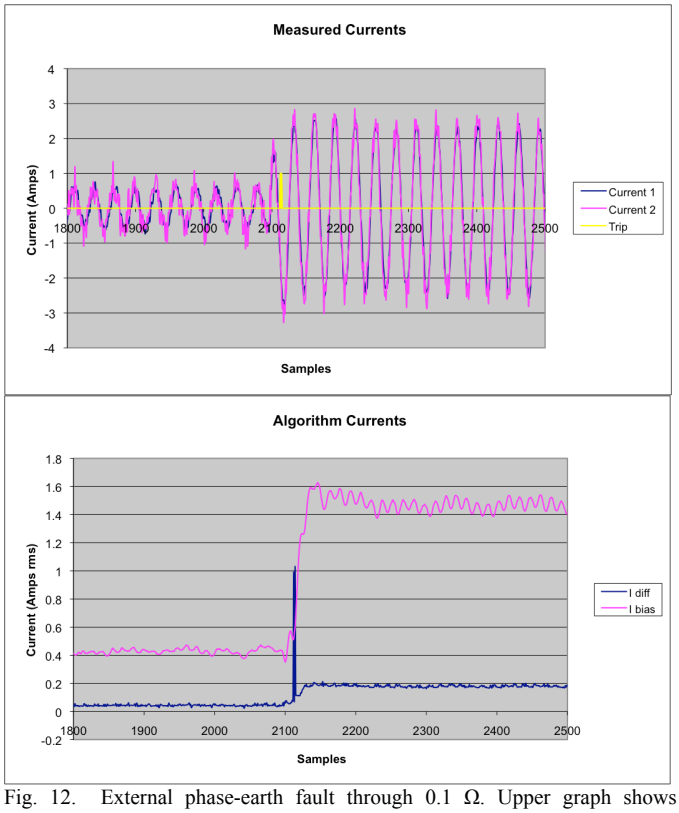

Fig. 12. External phase-earth fault through 0.1 Ω. Upper graph shows instantaneous currents and Trip comparator. Lower graph shows differential and bias currents.

V. Discussion

Measurement noise in these tests is due primarily to the mismatch between the operating ranges of CTs and piezoelectric stacks, which were retroactively matched for the purposes of this study. By redesigning the CT and stack to

match, this noise can be greatly reduced allowing both the sensitivity of the protection scheme and the maximum fault resistance to be increased.

Since the technology demonstrated here is capable of measuring both voltage and current, a particularly novel application of these transducers would be that of simultaneously measuring both these parameters and thus providing a point sensor for "apparent impedance". This would then enable the distributed measurement of impedance for use in a fibre-optic distance protection network. Such a system would be capable of simultaneous optical interrogation of a number of distance protection locations, each of which could be separated by up to 100 km of fibre, with all-optical signal boosting implemented at certain substation points using fibre amplifiers.

There are other potential protection/automation applications of distributed voltage and current measurements in power transmission and distribution networks, particularly those with high penetrations of embedded generation. The potential opportunities for novel methods for the protection of such "active networks" or "microgrids" warrant further investigation.

As an alternative to the use of CTs for conversion of current to a measurable voltage, magnetostrictive materials could be employed to enable the straining of fibre Bragg gratings directly by the magnetic field encircling a conductor. This would introduce the possibility of developing a clip-on, coil-free sensor module for current and voltage (when combined with the technology presented here) [5, 6]. This method would, however, introduce cross talk between closely spaced conductors or from any stray magnetic fields; an effect to which the technique described in this paper is immune.

VI. Conclusions

In this paper we have described the design and testing of an all-optical power systems protection network in differential current unit protection configuration and demonstrated its high performance over a range of fault scenarios and resistances. Further development of the technology will lead to field-ready packaged devices with reduced size and improved performance in terms of reduced noise and increased sensitivity.

The potential benefits of this system compared with existing technology include the interrogation distance (up to 100 km prior to signal amplification), the spectral-encoding of measurement information, the lack of a separate communications channel between measurement points, the inherent temperature-sensing capability of each transducer, and the ability to implement protection algorithms involving up to 30 separate current or voltage measurement points using only one addressing fibre.

The capability of the technology to measure both voltage and current over extended distances has clear application in distributed distance protection and in other novel methods for protection of power networks, particularly future networks where high numbers of distributed generation sources may be connected to the network.

Acknowledgements

This work was supported in part by Toshiba Corporation.

References

[1] AREVA T&D, *Network Protection and Automation Guide*. 1st Ed., Cayfosa, Barcelona, ISBN 2-9518589-0-6, July 2002.

[2] P. Niewczas, J. R. McDonald, "Advanced optical sensors for power and energy systems," *IEEE Instrumentation and Measurement Magazine*, vol. 10, no. 1, pp. 18–28, February 2007.

[3] K. Bonhert, P. Gabus, J. Kostovic, H. Brandle, "Optical fiber sensors for the electric power industry," *Optics and Lasers in Engineering (Elsevier)*, vol. 43, pp. 511–526, 2005.

[4] L. Dziuda, G. Fusiek, P. Niewczas, G. M. Burt, J. R. McDonald, "Laboratory evaluation of the hybrid fiber-optic current sensor," *Sensors and Actuators (Elsevier)*, vol. 136, pp 184–190, 2007.

[5] M. Sedlar, V. Matejec, I. Paulicka, "Optical fibre magnetic field sensors using ceramic magnetostrictive jackets," *Sensors and Actuators*, vol. 84, pp. 297–302, February 2000.

[6] D. Reilly, A. J. Willshire, G. Fusiek, P. Niewczas, J. R. McDonald, "A fiber-Bragg-grating-based sensor for simultaneous AC current and temperature measurement," *IEEE Sensors Journal*, vol. 6, no. 6, December 2006.